Hybrid Space Division Multiple Access and Quasi-Orthogonal Multiple Access for Multi-User Underwater Visible Light Communication

Yangping Qian, Chen Chen, *Member, IEEE*, Pengfei Du, and Min Liu

***Abstract*—Due to severe inter-beam interference and high cost of conventional full space division multiple access (SDMA)-based multi-user underwater visible light communication (MU-UVLC) systems, partial SDMA has been considered to substantially reduce inter-beam interference and costs by enabling closely located users to share the same light beam. Moreover, non-orthogonal multiple access (NOMA) is generally adopted to multiplex users in the same beam. However, for users with similar channel gains, the use of NOMA may suffer from severe error propagation. To this end, we propose and demonstrate a hybrid SDMA and quasi-orthogonal multiple access (QOMA) scheme for performance enhancement of partial SDMA-based MU-UVLC systems. Simulation and experimental results show that, in two-user UVLC system applying hybrid SDMA/QOMA, the bit error rate (BER) performance of the near user can be substantially improved and a much wider range of effective power allocation ratio can be achieved compared with that using conventional hybrid SDMA/NOMA.**

***Index Terms*—Underwater visible light communication, space division multiple access, quasi-orthogonal multiple access.**

I. Introduction

UNDERWATER visible light communication (UVLC) has attracted extensive attention in recent years due to its distinct advantages over traditional underwater acoustic and radio frequency (RF) communications, including large bandwidth, high data rate, low time latency, high security, and low power consumption [1]. As a result, UVLC has been widely considered as a promising communication technology for underwater environments [2]. To enable communication with multiple users simultaneously, multiple access techniques are of great significance for UVLC systems. More specifically, orthogonal multiple access (OMA) and non-orthogonal multiple access (NOMA) have already been used in UVLC systems [3], [4], [5], [6]. Moreover, space division multiple access (SDMA) has also been shown to be an efficient approach for supporting multiple users by utilizing multiple spatial channels in indoor VLC systems. For example, SDMA based optical beamforming by using a LED light and a spatial light modulator was reported in [7], angle diversity transmitter enabled SDMA was proposed in [8], and SDMA has been realized in multi-user multiple-input multiple-output VLC (MU-MIMO-VLC) systems [9], [10].

Lately, a hybrid SDMA/NOMA scheme has been adopted to support multiple users in UVLC systems in [11], where NOMA is used to serve the users covered by each light beam. It is well known that NOMA is generally advantageous only when users have distinctive channel conditions [12]. However, the users within the same light beam in SDMA-based MU-UVLC systems might have very similar channel conditions, and hence traditional NOMA might not achieve satisfactory performance gain due to the severe error propagation effect. In [13], a new NOMA scheme free of successive interference cancellation (SIC) has been proposed based on constellation division coding (CPC) and uneven constellation demapping (UCD), which can efficiently eliminate error propagation even users have very similar channel conditions. As a result, such a SIC-free NOMA scheme can be termed as quasi-orthogonal multiple access (QOMA).

In this article, for the first time, we propose and investigate a novel hybrid SDMA/QOMA scheme for MU-UVLC systems. By dividing the closely located users into groups, SDMA is used to support multiple user groups by configuring the same number of light beams, while QOMA is adopted to serve users with similar channel conditions within each light beam. Simulations and experiments have been conducted to verify the feasibility and superiority of the proposed hybrid SDMA/QOMA scheme over other benchmark schemes in MU-UVLC systems.

II. Principle

In this section, we first introduce the underwater channel model and then discuss the principle of the proposed hybrid SDMA/QOMA scheme for MU-UVLC systems. Finally, the principle of QOMA is also described.

A. Channel Model

Although UVLC has many technical benefits, its practical application in underwater environments still remains challenging due to the severe power attenuation of the received optical signal. Specifically, when photons from the incident beams propagate

Manuscript received 11 May 2023; revised 8 July 2023; accepted 20 July 2023. Date of publication 24 July 2023; date of current version 2 August 2023. This work was supported in part by the National Natural Science Foundation of China under Grant 62271091, in part by the Natural Science Foundation of Chongqing under Grant cstc2021jcyj-msxmX0480, and in part by Sichuan Provincial S&T Projects under Grant 2020YFH0054. *(Corresponding author: Chen Chen.)*

Yangping Qian, Chen Chen, and Min Liu are with the School of Microelectronics and Communication Engineering, Chongqing University, Chongqing 400044, China (e-mail: c.chen@cqu.edu.cn).

Pengfei Du is with the A*STAR's Singapore Institute of Manufacturing Technology, Singapore 138634 (e-mail: Du_Pengfei@simtech.astar.edu.sg).

Digital Object Identifier 10.1109/JPHOT.2023.3298337

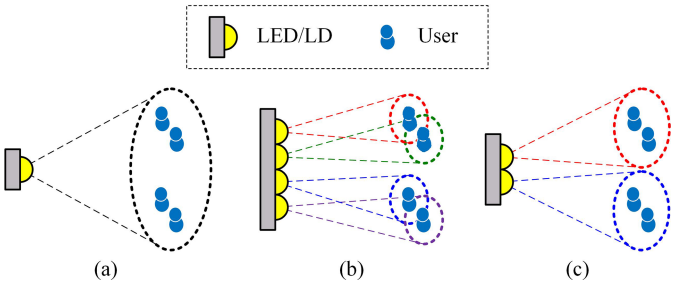

Fig. 1. Illustration of a MU-UVLC system using (a) single-beam broadcasting, (b) full SDMA, and (c) partial SDMA.

through water, they inevitably interact with water molecules or other suspended particles, leading to absorption and scattering phenomena that cause light attenuation and multi-path fading. Due to the adverse effects of absorption and scattering, the data rate and transmission distance of UVLC are still greatly limited. The light attenuation effects in underwater environment can be described by the Beer-Lambert Law, which provides a simple model as [2], [14]

$$I = I_0 \exp\left(-c(\lambda)d\right), \tag{1}$$

where I_0 and I respectively represent the light intensities at the transmitter side and the receiver side, d is the transmission distance, and $c(\lambda)$ denotes the total attenuation coefficient which can be given by

$$c(\lambda) = a(\lambda) + b(\lambda), \tag{2}$$

where $a(\lambda)$ and $b(\lambda)$ denote the absorption and scattering coefficients for underwater light propagation, respectively.

When the optical signal is transmitted in fresh water under the absence of turbulence, the channel gain h_{ij} for the line-of-sight (LOS) UVLC system can be defined as [15]

$$h_{ij} = \exp\left(-c(\lambda)d\right) \frac{(m+1)A}{2\pi d^2} \mu\eta \cos^m(\psi) \cos(\theta), \tag{3}$$

where $m = -\ln 2/\ln(\cos\Psi)$ represents the Lambertian emission order with Ψ being the semi-angle at half power of the transmitter, A is the effective receiving area of the receiver, and the gains of the optical filter and the optical lens are denoted by μ and η, respectively. Specifically, the gain of the optical lens is defined as $\eta = \frac{r^2}{\sin^2\Theta}$, where r and Θ represent the refractive index and the half-angle field-of view (FOV) of the optical lens, respectively. Moreover, ψ is the emission angle and θ is the incident angle.

In UVLC systems, the additive noise typically consists of background noise, shot noise and thermal noise, which can be commonly modeled as a real-valued zero-mean additive white Gaussian noise (AWGN) with power of $P_n = N_0 B$, where N_0 represents the noise power spectral density (PSD) and B denotes the signal bandwidth [2].

B. Hybrid SDMA/QOMA for MU-UVLC

In a typical MU-UVLC system, as shown in Fig. 1, multiple access can be performed mainly in the following ways: 1) single-beam broadcasting, 2) full SDMA and 3) partial SDMA.

TABLE I
COMPARISON OF MULTIPLE ACCESS SCHEMES IN MU-UVLC

Scheme	Single-beam broadcasting	Full SDMA	Partial SDMA
Beam divergence angle	large	small	relatively small
Received optical power	low	high	relatively high
Inter-beam interference	no	strong	negligible
Cost	low	high	relatively low

For single-beam broadcasting, as can be seen in Fig. 1(a), a single light beam is used to serve all the users and the received optical power of each user is low since the light beam has a large divergence angle. For full SDMA, as depicted in Fig. 1(b), each user is individually served by a light beam with a small divergence angle and hence can have a high received optical power. Nevertheless, the implementation of full SDMA requires multiple light-emitting diode/laser diode (LED/LD) transmitters to create light beams to serve the same number of users, which inevitably increase the overall cost of the MU-UVLC system, especially when there are a large number of users in the system. Moreover, when users are located near each other, the adjacent light beams might overlap with each other, resulting in strong inter-beam interference. For partial SDMA, as shown in Fig. 1(c), the users are first divided into groups and then each user group is allocated with one light beam. Compared with full SDMA, partial SDMA requires much fewer LED/LD transmitters to support the same number of users and thus the overall system cost is relatively low. By dividing the closely located users into groups when performing partial SDMA, the divergence angle of a light beam serving a user group can be relatively small. Hence, the received optical power of each user can be relatively high and the inter-beam interference can also be negligible. The comparison of different multiple access schemes in MU-UVLC systems is given in Table I.

According to the above comparison, we can see that partial SDMA is a trade-off between single-beam broadcasting and full SDMA, which is promising for the application in practical MU-UVLC systems. In MU-UVLC systems applying partial SDMA, users within the same light beam might have very similar channel conditions and hence traditional NOMA might work well in this case. Hence, a more efficient intra-beam multiple access scheme should be used to further enhance the performance of SDMA-based MU-UVLC systems.

Considering the channel similarity issue in each user group, we propose a hybrid SDMA/QOMA scheme for MU-UVLC systems, where SDMA is used for inter-beam multiple access while QOMA is used for intra-beam multiple access. More specifically, QOMA can be considered as an improved NOMA scheme which is capable of eliminating the adverse error propagation effect, which has been proposed in our previous work [13], and hence QOMA is very suitable to support users with similar channel conditions. The detailed principle of QOMA will be discussed in the following subsection.

In practical MU-UVLC systems, there might be more than two users closely distributed and a light beam might need to serve

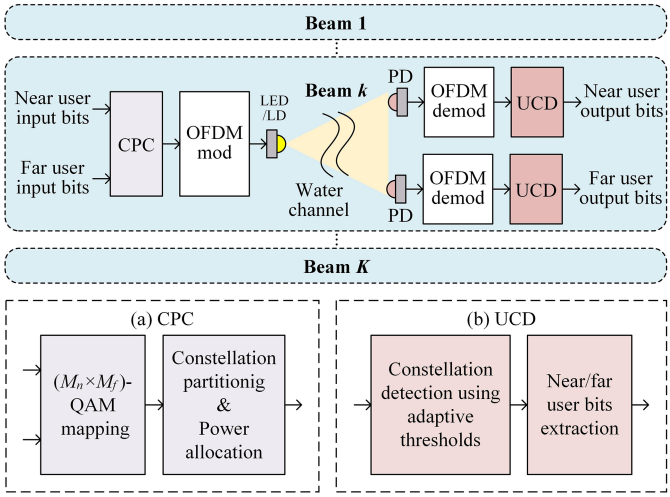

Fig. 2. Schematic diagram of a K-beam MU-UVLC system employing hybrid SDMA/QOMA. Insets (a) and (b) show the principles of CPC and UCD, respectively.

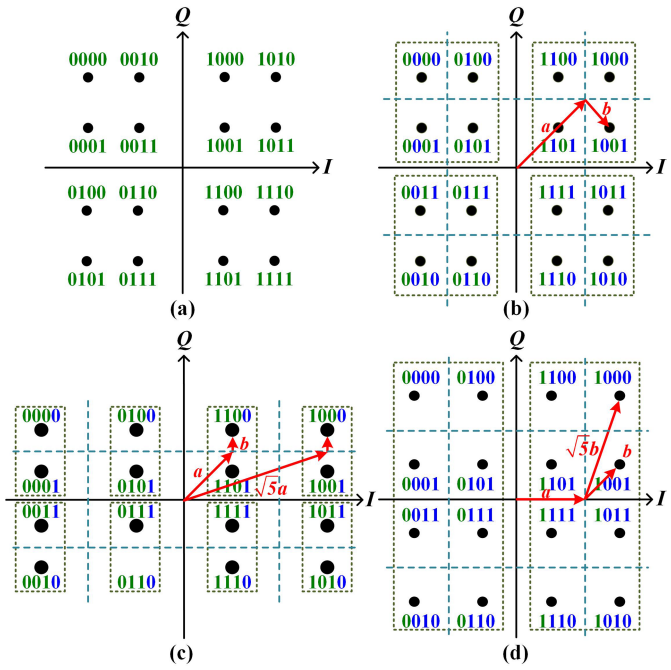

Fig. 3. (a) Non-Gray-coded 16-QAM constellation generated by SPC and Gray-coded 16-QAM constellation generated by CPC for (b) $b_n = b_2b_4$, $b_f = b_1b_3$, (c) $b_n = b_4$, $b_f = b_1b_2b_3$, and (d) $b_n = b_2b_3b_4$, $b_f = b_1$.

more than two users. For the case that there are more than two users within a light beam, these users can be first sorted based on their channel gains and then divided into pairs. Subsequently, NOMA or QOMA can be adopted to support the two users within each user pair, while orthogonal frequency division multiple access (OFDMA) can be used to support different user pairs. Please refer to our previous work [16] for more details. As a result, for simplicity and without loss of generality, each light beam is assumed to serve two users in the following analysis and evaluations.

Fig. 2 illustrates the schematic diagram of a K-beam MU-UVLC system employing hybrid SDMA/QOMA, where each light beam serves two users including a near user and a far user. As we can see, the input bits of the near and far users in each light beam are first processed via CPC and then orthogonal frequency division multiplexing (OFDM) modulation is performed to obtain a non-negative real-valued output signal to modulate the light intensity of the corresponding LED/LD transmitter. After propagation through the water channel, the optical signal is detected by the photo-detector (PD) of each user. The resultant electrical OFDM signal of each user is first demodulated and then UCD is executed to recover the corresponding output bits.

C. QOMA Enabled by CPC and UCD

Differing from traditional NOMA which is based on superposition coding (SPC) and SIC, the adopted QOMA is enabled by CPC and UCD [13]. The principle of CPC is shown in Fig. 2(a), where the input bits of the near user and the far user are first mapped into a Gray-coded $(M_n \times M_f)$-ary quadrature amplitude modulation (QAM) constellation symbol, with M_n and M_f representing the required modulation orders for the near user and the far user, respectively. Subsequently, the Gray-coded QAM constellation is divided into several sub-constellations according to the bit allocation scheme between the near and far users, and then power allocation is conducted to reshape the constellation. Moreover, the principle of UCD is shown in Fig. 2(b), where the obtained constellation symbols after OFDM modulation are demapped to recover the output bit sequence by using adaptive thresholds which can be derived according to the adopted power allocation ratio. Finally, the output bits of each user can be extracted from the output bit sequence directly according to the adopted bit allocation scheme. In the following, we take the 16-QAM constellation as an example to introduce hybrid SDMA/QOMA. In fact, the general rule of hybrid SDMA/QOMA is applicable to the QAM constellation with an arbitrary order, i.e., the values of M_n and M_f can be arbitrary. In practical systems, we can choose a suitable QAM constellation based on the quality-of-service (QoS) requirements of different users.

Fig. 3(a) depicts the non-Gray-coded 16-QAM constellation generated by traditional SPC, where adjacent two constellation points on both sides of the I axis or the Q axis generally have a two-bit difference. In contrast, for the Gray-coded 16-QAM constellation generated by CPC, as shown in Fig. 3(b), (c) and (d), there is only a one-bit difference between any of the two adjacent constellation points. As a result, the CPC-generated Gray-coded 16-QAM constellation can efficiently eliminate the adverse error propagation effect and hence have a much better error performance in comparison to the SPC-generated non-Gray-coded 16-QAM constellation. Moreover, for the CPC-generated Gray-coded 16-QAM constellation with each constellation point carrying four bits, there are three ways to partition the overall constellation into sub-constellations, which correspond to three bit allocation schemes among the near and far users.

Let b_n and b_f denote the bit/bits allocated to the near and far users, respectively. When both the near and far users are allocated with two bits, i.e., $b_n = b_2b_4$ and $b_f = b_1b_3$, as shown

in Fig. 3(b), the 16-QAM constellation is divided into four 4-QAM sub-constellations, and the power allocation ratio (PAR) between the far user and near user can be expressed by

$$\rho_1 = \frac{a^2}{b^2}. \tag{4}$$

When the near user is allocated with one bit and the far user is allocated with three bits, i.e., $b_n = b_4$ and $b_f = b_1 b_2 b_3$, as shown in Fig. 3(c), the 16-QAM constellation is divided into eight binary phase-shift keying (BPSK) sub-constellations, and the PAR between the far user and near user can be obtained by

$$\rho_2 = \frac{a^2 + 5a^2}{2b^2} = \frac{3a^2}{b^2}. \tag{5}$$

Similarly, when the near user is allocated with three bits and the far user is allocated with one bit, i.e., $b_n = b_4$, $b_f = b_1 b_2 b_3$, as can be seem from Fig. 3(d), the 16-QAM constellation is divided into two 8-QAM sub-constellations, and the PAR between the far user and near user can be achieved by

$$\rho_3 = \frac{2a^2}{b^2 + 5b^2} = \frac{a^2}{3b^2}. \tag{6}$$

Due to the constellation reshaping through power allocation at the transmitter side, adaptive thresholds need to be used for constellation demapping at the receiver side. As can be observed from Fig. 3(b), (c) and (d), the adaptive thresholds to perform UCD for three different bit allocation schemes can be expressed as follows:

$$\begin{cases} \left\{I = 0, \pm\frac{a}{\sqrt{2}}; Q = 0, \pm\frac{a}{\sqrt{2}}\right\}, & \text{if } b_n = b_2 b_4, b_f = b_1 b_3 \\ \left\{I = 0, \pm\sqrt{2}a; Q = 0, \pm\frac{a}{\sqrt{2}}\right\}, & \text{if } b_n = b_4, b_f = b_1 b_2 b_3 \\ \left\{I = 0, \pm a; Q = 0, \pm\sqrt{2}b\right\}, & \text{if } b_n = b_2 b_3 b_4, b_f = b_1 \end{cases}. \tag{7}$$

III. Results and Discussions

In this section, we perform numerical simulations and hardware experiments to evaluate and compare the performance of the proposed hybrid SDMA/QOMA scheme in practical MU-UVLC systems.

A. Simulation Results

In the simulations, we consider an OFDM-based UVLC system with four users utilizing different multiple access schemes, where we assume the signals are transmitted through a pure seawater channel and hence the overall attenuation coefficient $c(\lambda)$ is set to 0.056 [14]. The separation between the transmitter and receivers is 10 m, and the transmitter semi-angles at half power for full SDMA, partial SDMA and single-beam broadcasting are set to 4°, 10° and 30°, respectively. Moreover, the length of inverse fast Fourier transform/fast Fourier transform (IFFT/FFT) is set to 256 and a total of 100 (i.e., 2nd to 101st) subcarriers are used for data transmission. The other simulation parameters can be found in Table II.

Fig. 4 illustrates the simulation average BER versus transmitted signal-to-noise (SNR) of the MU-UVLC system applying single-beam broadcasting, partial SDMA and full SDMA. In the case of full SDMA, when users are located close to each other or there are some fluctuations in the seawater, the optical beam serving an independent user may overlap with adjacent beams, resulting in severe inter-beam interference for adjacent users. It can be clearly seen from Fig. 4 that full SDMA performs the best among all the schemes when there is no interference. However, in the presence of interference, the BER performance of full SDMA deteriorates significantly and a BER floor above the 7% forward error correction (FEC) coding limit of 3.8×10^{-3}. Furthermore, the widespread implementation of full SDMA might be impractical due to its high cost, especially in scenarios with a large number of users. In contrast, partial SDMA offers a promising solution by not only significantly reducing system deployment cost but also greatly outperforming single-beam broadcasting and full SDMA with interference, which can achieve a trade-off between overall cost and system performance. Therefore, partial SDMA emerges as a favorable choice for practical MU-UVLC systems.

In the next, we investigate the BER performance of the partial SDMA-based two-user UVLC system applying NOMA and QOMA. Fig. 5(a)–(c) depict the simulation BER versus PAR for three bit allocation schemes. As we can see, the BER for the far users remain almost the same and gradually decrease with the increase of PAR. However, for the near user, as the PAR increases,

TABLE II
Simulation Parameters

Parameter	Value
Attenuation coefficient	0.056
Separation between the transmitter and receivers	10 m
Tx semi-angle at half power for full SDMA	4°
Tx semi-angle at half power for partial SDMA	10°
Tx semi-angle at half power for single-beam broadcasting	30°
Gain of optical filter	0.9
Refractive index of optical lens	1.5
Half-angle FOV of optical lens	60°
Responsivity of PD	0.53 A/W
Active area of PD	1 cm^2
Signal bandwidth	20 MHz
Noise spectral density	$10^{-22} A^2/Hz$
IFFT/FFT length	256
Number of data subcarriers	100

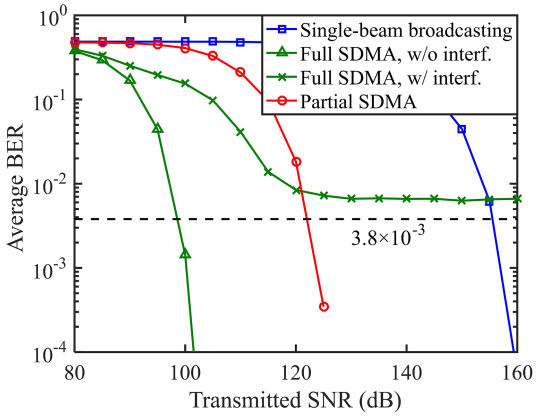

Fig. 4. Average BER vs. transmitted SNR for single-beam broadcasting, partial SDMA, full SDMA without and with interference (w/o: without, w/: with, interf.: interference).

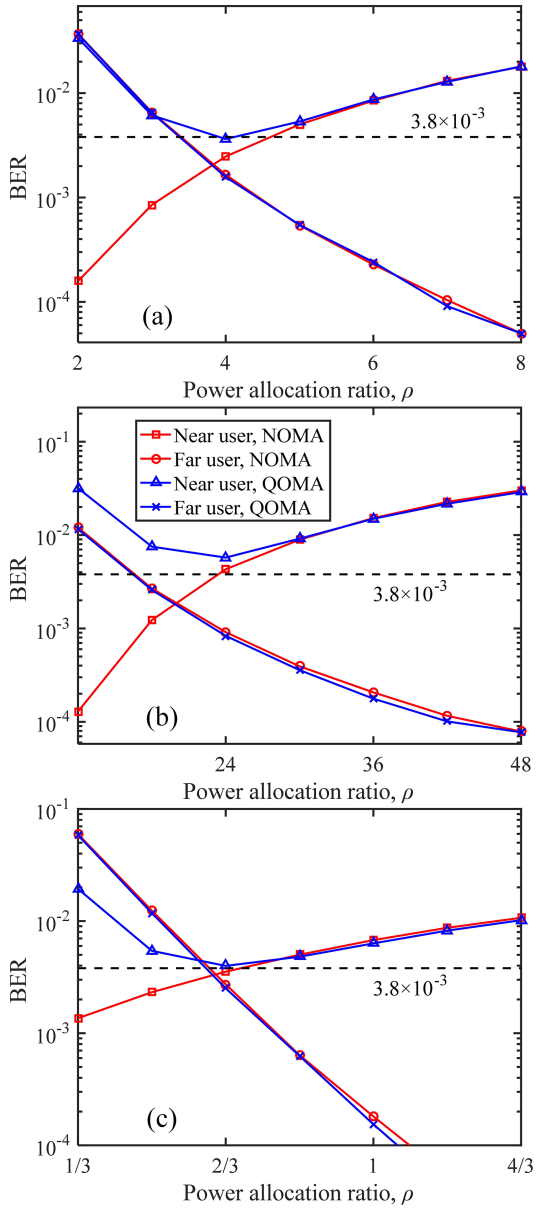

Fig. 5. Simulation BER vs. power allocation ratio ρ for 16-QAM constellation with (a) $b_n = b_2b_4$, $b_f = b_1b_3$, (b) $b_n = b_4$, $b_f = b_1b_2b_3$, (c) $b_n = b_2b_3b_4$, $b_f = b_1$.

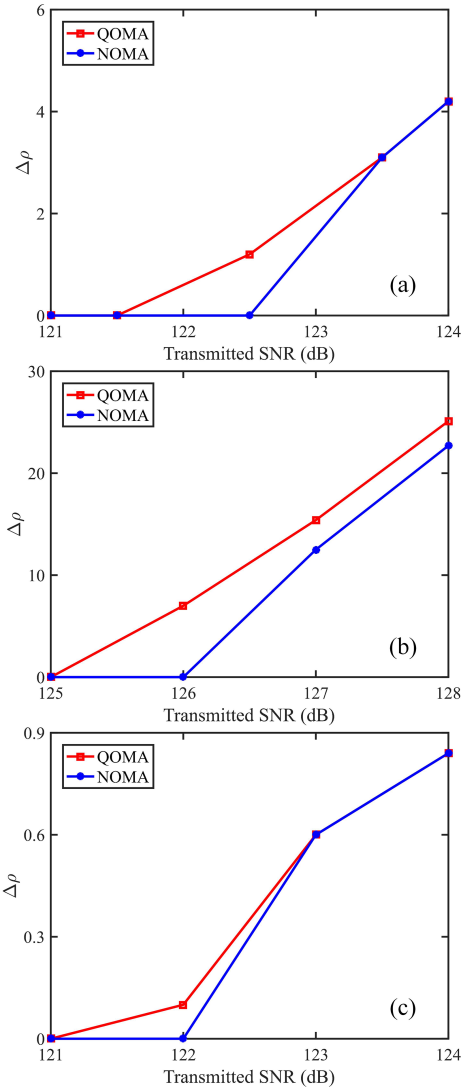

Fig. 6. Simulation $\Delta\rho$ vs. the transmitted SNR for 16-QAM constellation with (a) $b_n = b_2b_4$, $b_f = b_1b_3$, (b) $b_n = b_4$, $b_f = b_1b_2b_3$, and (c) $b_n = b_2b_3b_4$, $b_f = b_1$.

the allocated power decreases, leading to an increased BER for QOMA and a decreased-then-increased BER for NOMA. It can be further observed that QOMA outperforms NOMA for the near user especially when the PAR is small. Therefore, applying QOMA in a partial SDMA-based MU-UVLC system can achieve better BER performance than conventional NOMA. Furthermore, it is worth noting that the near user fails to reach BER $= 3.8 \times 10^{-3}$ at low transmitted SNR when using NOMA. In contrast, both users exhibit reliable BER performance within a specific range of PAR values when applying QOMA.

Fig. 6(a)–(c) show the simulation $\Delta\rho$ versus transmitted SNR for the three bit allocation schemes, where $\Delta\rho$ is defined as the range value of the PAR within which both users can reach the FEC limit of 3.8×10^{-3}. It has been shown that a wider range enables a greater flexibility in resource scheduling by adjusting the PAR value to meet the BER requirements of users. As shown in Fig. 6, $\Delta\rho$ achieved by both QOMA and NOMA increases with the increase of the transmitted SNR. Moreover, $\Delta\rho$ achieved by QOMA is always larger or equal to that achieved by NOMA for all the three bit allocation schemes. Particularly, as shown in Fig. 6(b), QOMA achieves the largest $\Delta\rho$ gain over NOMA due to the severe error propagation caused by the higher modulation order of the far user. Therefore, QOMA is an efficient approach for expanding the range of effective PAR in the partial SDMA-based two-user UVLC system, especially when the far user has a higher modulation order.

B. Experimental Results

In this section, we further experimentally evaluate and compare the performance of the proposed hybrid SDMA/QOMA scheme in a practical MU-UVLC system using commercially

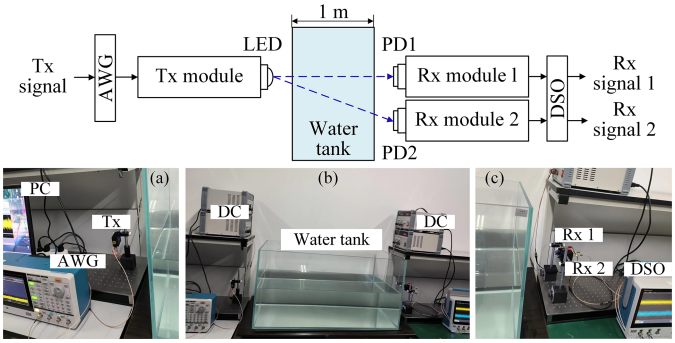

Fig. 7. Experimental setup of the two-user UVLC system using commercially available Tx and Rx modules. Insets: photo of (a) the transmitter part, (b) the overall system, and (c) the receiver part.

TABLE III
EXPERIMENTAL PARAMETERS

Parameter	Value
AWG sampling rate	250 MSa/s
DC voltage	12 V
Tx peak-to-peak voltage	250 mV
Tx wavelength	459.3 nm
Tx optical power	18.5 mW
Rx active area	φ1.5 mm
Rx output gain	14 dB
Rx cutoff frequency	230 MHz
MDO sampling rate	1.25 GSa/s
Modulation scheme	16-QAM
IFFT/FFT size	256
Transmission distance	100 ∼120 cm

available transmitter (Tx) and receiver (Rx) modules. The Tx/Rx modules used in this experiment are highly integrated modules and more details about these modules can be found in [17]. Due to the hardware limitations, we consider a single-beam two-user UVLC system to investigate and compare the performance of partial SDMA using NOMA and QOMA. The experimental setup is depicted in Fig. 7, where the transmitted signal generated offline by MATLAB is first loaded to an arbitrary waveform generator (AWG, Tektronix AFG31102) with a sampling rate of 250 MSa/s. Then, the output signal of AWG is sent to the Tx module (HCCLS2021MOD01-Tx), which is driven by a 12-V DC voltage. During OFDM modulation, the length of IFFT/FFT is 256 and the signal bandwidth is dynamically adjusted by allocating different number of subcarriers for data transmission, i.e., N_{data}. After passing through a 1-m water tank filled with tap water, the optical signal is detected by two users each equipped with a Rx module (HCCLS2021MOD01-Rx), where the near user faces the LED and the far user is located next to the near user. Subsequently, the detected signals are recorded by a two-channel digital storage oscilloscope (DSO, Tektronix MDO32) with a sampling rate of 1.25 GSa/s, which are further processed offline by MATLAB. The insets (a), (b) and (c) in Fig. 7 show the photos of the transmitter part, the overall system and the receiver part, respectively. The experimental parameters of the two-user UVLC system using commercially available Tx and Rx modules are listed in Table III.

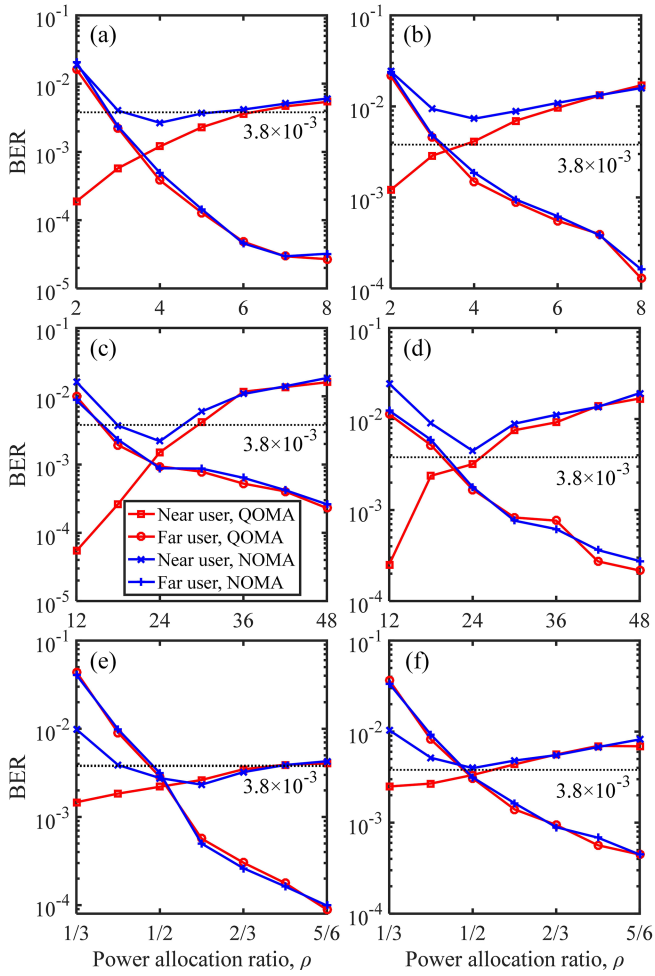

Fig. 8. Measured BER vs. power allocation ratio ρ for 16-QAM constellation with (a) $b_n = b_2b_4$, $b_f = b_1b_3$ and $N_{\text{data}} = 68$, (b) $b_n = b_2b_4$, $b_f = b_1b_3$ and $N_{\text{data}} = 72$, (c) $b_n = b_4$, $b_f = b_1b_2b_3$ and $N_{\text{data}} = 54$, (d) $b_n = b_4$, $b_f = b_1b_2b_3$ and $N_{\text{data}} = 58$, (e) $b_n = b_2b_3b_4$, $b_f = b_1$ and $N_{\text{data}} = 74$, and (f) $b_n = b_2b_3b_4$, $b_f = b_1$ and $N_{\text{data}} = 77$.

Fig. 8 shows the measured BER versus the PAR for 16-QAM constellation with three bit allocation schemes. For all the cases, the BER of NOMA and QOMA is almost the same for the far user, which gradually decreases with the increase of PAR. However, for the near user, QOMA can achieve better BER performance than NOMA. With increasing PAR, the BER of the near user using NOMA initially decreases and then gradually increases. Specifically, when the PAR is small, the BER of the near user with NOMA is much higher than with QOMA due to adverse error propagation effect. Nevertheless, when the PAR is relatively large, the error propagation is slight, resulting in an extremely similar BER of the near user with QOMA and NOMA. Hence, the BER performance of the near user is robust against the interference from the far user with QOMA. As a result, QOMA can greatly improves the near user's BER especially at low PAR in a practical partial SDMA-based two-user UVLC system.

Furthermore, we define the effective PAR ρ_e as the value of ρ that the BER of both users is below the 7% FEC requirement of 3.8×10^{-3}. For the case shown in Fig. 8(a) that $b_n = b_2b_4$

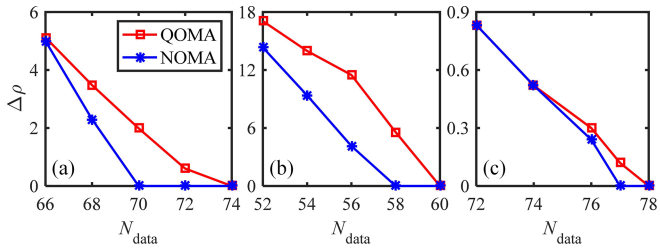

Fig. 9. Measured $\Delta\rho$ vs. the number of data subcarriers N_{data} for 16-QAM constellation with (a) $b_n = b_2b_4$, $b_f = b_1b_3$, (b) $b_n = b_4$, $b_f = b_1b_2b_3$, and (c) $b_n = b_2b_3b_4$, $b_f = b_1$.

and $b_f = b_1b_3$, when using 68 (i.e., 2nd to 69th) subcarriers to modulate data with a bandwidth of about 66.4 MHz, the range of ρ_e achieved by NOMA is (3.14, 5.44), while QOMA extends the range to (2.73, 6.21). Similarly, for $b_n = b_4$ and $b_f = b_1b_2b_3$ with $N_{\text{data}} = 54$ in Fig. 8(c), the range of ρ_e is extended from (17.92, 27.29) to (15.52, 29.49) when NOMA is replaced by QOMA. For $b_n = b_2b_3b_4$ and $b_f = b_1$ with $N_{\text{data}} = 74$, Fig. 8(e) shows that both NOMA and QOMA yield a ρ_e range of (0.63, 1.15). Moreover, as shown in Fig. 8(b), (d) and (f), with more subcarriers used to modulate data, the range of ρ_e is 0 with NOMA, and the QOMA extends the range to (3.17, 3.77), (19.64, 25.21) and (0.63, 0.75), respectively. The results show that the range of ρ_e is significantly expanded by QOMA.

Fig. 9 depicts the measured $\Delta\rho$ versus the number of data subcarriers for 16-QAM constellation with three bit allocation schemes. As we can see, $\Delta\rho$ is gradually reduced with the increase of N_{data}, eventually reaching 0 for QOMA and NOMA, which is mainly because a larger system bandwidth results in a poorer BER performance for both users. Furthermore, for $b_n = b_4$, $b_f = b_1b_2b_3$ as in Fig. 9(b), the $\Delta\rho$ values are 4.1 and 11.5 for NOMA and QOMA with $N_{\text{data}} = 56$, respectively, which indicates an 180.5% extension of $\Delta\rho$ by using QOMA over NOMA. Moreover, as the modulation order of the far user increases, the advantage of QOMA becomes more significant due to the increased severity of error propagation. Therefore, the efficient application of QOMA can achieve better performance and significantly increase the range of effective PAR, which makes it possible to support higher data rate transmission for partial SDMA-based MU-UVLC systems.

IV. Conclusion

In this article, we have proposed and experimentally demonstrated a hybrid SDMA/QOMA scheme for practical MU-UVLC systems. Compared with conventional transmission schemes, the hybrid SDMA/QOMA scheme can not only obtain relatively high received optical power, but also have relatively low cost and negligible inter-beam interference. Moreover, QOMA is applied to enhance the performance of partial SDMA-based MU-UVLC systems, since QOMA can eliminate the adverse error propagation effect under channel similarity. The simulation and experimental results show that the efficient application of hybrid SDMA/QOMA not only achieves excellent BER performance compared with single-beam broadcasting and full SDMA with interference, but also outperforms conventional hybrid SDMA/NOMA. More specifically, hybrid SDMA/QOMA can significantly improve the BER for the near user and hence substantially extend the effective PAR range, especially when the far user has a large modulation order. Therefore, the proposed hybrid SDMA/QOMA scheme can be a promising candidate to support multiple users in practical MU-UVLC systems.

References

[1] S. Arnon, "Underwater optical wireless communication network," *Proc. SPIE*, vol. 49, no. 1, Jan. 2010, Art. no. 015001.
[2] Z. Zeng, S. Fu, H. Zhang, Y. Dong, and J. Cheng, "A survey of underwater optical wireless communications," *IEEE Commun. Surveys Tuts.*, vol. 19, no. 1, pp. 204–238, First Quarter 2017.
[3] M. Elamassie, M. Karbalayghareh, F. Miramirkhani, M. Uysal, M. Abdallah, and K. Qaraqe, "Resource allocation for downlink OFDMA in underwater visible light communications," in *Proc. Int. Black Sea Conf. Commun. Netw.*, 2019, pp. 1–6.
[4] D. Chen, Y. Wang, J. Jin, H. Lu, and J. Wang, "An experimental study of NOMA in underwater visible light communication system," *Opt. Commun.*, vol. 475, Nov. 2020, Art. no. 126199.
[5] L. Zhang et al., "Towards a 20 Gbps multi-user bubble turbulent NOMA UOWC system with green and blue polarization multiplexing," *Opt. Exp.*, vol. 28, no. 21, pp. 31796–31807, Oct. 2020.
[6] L. Bariah, M. Elamassie, S. Muhaidat, P. C. Sofotasios, and M. Uysal, "Non-orthogonal multiple access-based underwater VLC systems in the presence of turbulence," *IEEE Photon. J.*, vol. 14, no. 1, Feb. 2022, Art. no. 7308707.
[7] S.-M. Kim and H.-J. Lee, "Visible light communication based on space-division multiple access optical beamforming," *Chin. Opt. Lett.*, vol. 12, no. 12, Dec. 2014, Art. no. 120601.
[8] Z. Chen, D. A. Basnayaka, and H. Haas, "Space division multiple access for optical attocell network using angle diversity transmitters," *J. Lightw. Technol.*, vol. 35, no. 11, pp. 2118–2131, Jun. 2017.
[9] C. Chen, Y. Yang, X. Deng, P. Du, and H. Yang, "Space division multiple access with distributed user grouping for multi-user MIMO-VLC systems," *IEEE Open J. Commun. Soc.*, vol. 1, pp. 943–956, 2020.
[10] C. Chen et al., "Hybrid 3DMA for multi-user MIMO-VLC," *J. Opt. Commun. Netw.*, vol. 14, no. 10, pp. 780–791, Oct. 2022.
[11] Y. Li, S. A. H. Mohsan, X. Chen, R. Tehseen, S. Li, and J. Wang, "Research on power allocation in multiple-beam space division access based on NOMA for underwater optical communication," *Sensors*, vol. 23, no. 3, Feb. 2023, Art. no. 1746.
[12] H. Marshoud, V. M. Kapinas, G. K. Karagiannidis, and S. Muhaidat, "Non-orthogonal multiple access for visible light communications," *IEEE Photon. Technol. Lett*, vol. 28, no. 1, pp. 51–54, Jan. 2016.
[13] C. Chen, W.-D. Zhong, H. Yang, P. Du, and Y. Yang, "Flexible-rate SIC-free NOMA for downlink VLC based on constellation partitioning coding," *IEEE Wireless Commun. Lett.*, vol. 8, no. 2, pp. 568–571, Apr. 2019.
[14] C. Geldard, J. Thompson, and W. O. Popoola, "A study of non-orthogonal multiple access in underwater visible light communication systems," in *Proc. IEEE Veh. Technol. Conf.*, 2018, pp. 1–6.
[15] A. Kumar and D. N. K. Jayakody, "Secure NOMA-assisted multi-LED underwater visible light communication," *IEEE Trans. Veh. Technol.*, vol. 71, no. 7, pp. 7769–7779, Jul. 2022.
[16] C. Chen, S. Fu, X. Jian, M. Liu, X. Deng, and Z. Ding, "NOMA for energy-efficient LiFi-enabled bidirectional IoT communication," *IEEE Trans. Commun.*, vol. 69, no. 3, pp. 1693–1706, Mar. 2021.
[17] C. Chen, Y. Nie, X. Zhong, M. Liu, and B. Zhu, "Characterization of a practical 3-m VLC system using commercially available Tx/Rx modules," in *Proc. Asia Commun. Photon. Conf.*, 2021, pp. 1–3.